Optimization of conventional Fenton and ultraviolet-assisted oxidation processes for the treatment of reverse osmosis retentate from a paper mill

Daphne Hermosilla [*], Noemí Merayo, Ruth Ordóñez and Ángeles Blanco

[a] *Department of Chemical Engineering, Complutense University of Madrid, Facultad de Ciencias Químicas, Ciudad Universitaria s/n, 28040 Madrid, Spain.*

[*] Corresponding author:

Tel.: +34 91 394 4645; fax: +34 91 394 4243

E-mail address: dhermosilla@quim.ucm.es (D. Hermosilla)

Abstract

According to current environmental legislation concerned with water scarcity, paper industry is being forced to adopt a zero liquid effluent policy. In consequence, reverse osmosis (RO) systems are being assessed as the final step of effluent treatment trains aiming to recover final wastewater and reuse it as process water. One of the most important drawbacks of these treatments is the production of a retentated stream, which is usually highly loaded with biorecalcitrant organic matter and inorganics; and this effluent must meet current legislation stringent constraints before being ultimately disposed. The treatment of biorefractory RO retentate from a paper mill by several promising advanced oxidation processes (AOPs) -conventional Fenton, photo-Fenton and photocatalysis- was optimized considering the effect and interaction of reaction parameters; particularly using response surface methodology (RSM) when appropriate (Fenton processes). The economical cost of these treatments was also comparatively assessed. Photo-Fenton process was able to totally remove the COD of the retentate, and resulted even operatively cheaper at high COD removal levels than conventional Fenton, which achieved an 80% reduction of the COD at best. In addition, although these optimal results were produced at pH = 2.8, it was also tested that Fenton processes are able to achieve good COD reduction efficiencies (> 60%) without adjusting the initial pH value, provided the natural pH of this wastewater was close to neutral. Finally, although TiO_2-photocatalysis showed the least efficient and most expensive figures, it improved the biodegradability of the retentate, so its combination with a final biological step almost achieved the total removal of the COD.

Keywords: Advanced oxidation processes; Fenton; photo-Fenton; photocatalysis; reverse osmosis retentate; paper mill effluents; response surface methodology.

1. Introduction

Reducing water use is considered among current most important environmental issues in pulp and paper industries (Ordoñez et al., 2009), which are adopting zero liquid effluent policies, including the closure of water circuits (Koppol et al., 2004), to minimize the use of fresh water. As a result of implementing such management policies, the water consumption within the paper sector has decreased much worldwide. In fact, the generation of wastewater has been significantly reduced from 46 m^3/t of paper in 1974 (Mobius and Helble, 2004) to around current 15 m^3/t (Sundholm, 2000). Examples of actual current fresh water consumption figures in some paper mills are: 0-4 m^3/t of packaging paper, and 8-16 m^3/t of newsprint, printing paper, tissue paper, or market pulp (BREF, 2011).

As high water quality is required for replacing fresh water use in some stages of the paper mill, like high pressure showers, reverse osmosis (RO) systems are being implemented as the final step of different treatment trains aiming to recover the final effluent from the mill and reuse it as process water. Although RO filtration ensures an almost total conductivity reduction and the removal of all pathogens (Asano and Cotruvo, 2004), its wider application is still limited by technical and financial challenges related to the disposal of the retentate (Greenlee et al., 2010a). Even though much research effort has been successfully devoted to reduce the generated retentate increasing the recovery efficiency of RO systems (e.g. Greenlee et al., 2010a and 2010b; Ning and Troyer, 2009), this trend inevitably results in a progressive higher concentration of pollutants in the retentated fraction, making more difficult meeting effluent discharge thresholds without performing a properly designed wastewater treatment previously.

Provided biological treatments are not able to remove biorecalcitrant compounds, which are usually present in this type of industrial effluent at high concentration levels (Ordoñez et al., 2010), new alternative technologies are called to integrate current treatment trains. Particularly, advanced oxidation processes (AOPs) have been shown able to successfully remove such biorecalcitrant substances. Achieving a partial oxidation of non biodegradable organics (e.g. lignin and chlorinated structures) increases wastewater biodegradability enough to perform further successful biological treatment (Amat et al., 2005).

Fenton process is one of the most common AOPs used for wastewater treatment because it is usually very efficient and implies a lower economical cost than others (e.g. Esplugas et al., 2002). Regardless a high COD removal efficiency could be achieved and its relative environmental friendliness, the Fenton treatment of wastewater is limited by the final production of iron sludge, which requires ultimate disposal (Pignatello et al., 2006). In order to minimize the generation of iron sludge adding just a catalytic ferrous iron content that is photo-recovered (Hermosilla et al., 2009b), the conventional Fenton process may be positively assisted by the application of UV-light, which furthermore enables the treatment of carboxylates by photo-decarboxylation (Hermosilla et al., 2009a).

On the other hand, recent research progress has been addressed on the application of reusable catalysts in UV-assisted AOPs, such as photocatalytic processes performed with titanium dioxide (TiO_2) (e.g. Chong et al., 2010). Particularly, heterogeneous photocatalysis catalyzed by TiO_2 has been shown to efficiently remove colour and dissolved organic carbon (DOC) from ECF bleaching effluents and other solutions containing lignin. In addition, a rapid decrease of toxicity has been also

reported for different solutions (Catalkaya and Kargi, 2007; Chang et al., 2004); as well as biodegradability may be enhanced enough to consider these photocatalytic processes as interesting pre-oxidation steps preceding biological treatment (Oller et al., 2011).

In short, the potential application of optimized conventional Fenton and photo-assisted oxidation processes, whether using Fe^{2+} or TiO_2 as catalyst, as novel promising alternatives for the treatment of the biorecalcitrant organic fraction present in RO retentate from a recovered paper mill is going to be assessed next.

2. Material and methods

2.1. Material and analytical methods

RO retentate was sampled from the last treatment step of a pilot plant placed inside a newsprint paper mill located in Madrid (Spain) that uses 100% recovered paper as raw material. This pilot trial was performed aiming to assess the feasibility of reclaiming the current paper mill effluent and reuse it within the process. The pilot plant combined biological (anaerobic + aerobic) and membrane filtration (UF + RO) technologies to treat wastewater flowing out from a dissolved air flotation unit placed in the first water loop of the deinking plant, which is the most contaminated stream of the paper mill.

The sampled RO retentate, which main analytical characteristics are shown in Table 1, was preserved in polyethylene bottles protected from light inside a refrigerator at 4 ± 1 ºC. Mid-strength biorefractory organic and inorganic loads characterized the sample (Table 1), as expected for this type of waste stream (Ordóñez et al., 2010). Sample preservation, all analyses, and measurements described next were performed according to the standard methods for the examination of water and wastewaters

(APHA, AWWA and WPCF, 2005). All used chemicals were of analytical grade and were supplied by PANREAC S.A. (Barcelona, Spain).

Chemical oxygen demand (COD) was measured by the colorimetric method at 600 nm using an Aquamate spectrophotometer (Thermo Scientific AQA 091801, Waltham, USA). A TOC analyzer (Apollo 9000, Tekmar Dohrmann, Ohio, USA) was used to measure total organic carbon (TOC) by the combustion infrared method. H_2O_2 concentration was determined using the titanium sulphate spectrophotometric method (Pobiner, 1961). Fe^{2+} concentration was determined using the 1,10-phenanthroline colorimetric method (Tamura et al., 1974); using ammonium fluoride as masking agent for ferric iron (Fe^{3+}) to avoid its potential interference in the measure. Total soluble iron concentration was measured reducing Fe^{3+} to Fe^{2+} iron adding hydroxylamine under acidified conditions, and then determining Fe^{2+} concentration as just described. pH was adjusted adding 1M H_2SO_4 or 1N NaOH when required.

2.2. Experimental procedures

2.2.1. Fenton process

The total solution volume in the reactor was 2 L. The sample to be treated was mixed inside using a magnetic device, and the temperature was adjusted to the desired value with a water heating and circulating device. The following operational reaction parameters were optimized following the methodology described next in the experimental design section: pH, reagent concentrations and reaction time. Considering that it has been reported that a change in temperature from 25ºC to 45ºC does not significantly affect the removal of COD in the Fenton treatment of other wastewater (Hermosilla et al., 2009b; Kang and Hwang, 2000; Rivas et al., 2005; Zhang et al.,

2005), reaction temperature was set at 25 ºC to avoid an unnecessary consumption of heating energy, provided this value is approximately the natural temperature at which RO retentate was sampled (Table 1).

Ferrous sulphate ($FeSO_4$) was added to reach the targeted Fe^{2+} concentration after the initial pH value was adjusted, which was thereafter monitored but not further controlled along the treatment. H_2O_2 was then added in batch mode until the desired concentration was reached. Fe^{2+} and total iron concentration, total COD, soluble COD, and soluble TOC were measured just before the addition of H_2O_2, which was considered as reaction time = 0. Aliquots of treated solution were periodically sampled with a syringe thereafter. These samples were neutralized to pH ≈ 9.00 adding 40% sodium hydroxide (NaOH), and then centrifuged during 15 min at 2000 rpm. COD, TOC, H_2O_2 concentration, and turbidity were measured in the collected supernatant. H_2O_2 concentration values were used to correct COD values according to Hermosilla et al. (2009b). Treatments were run until H_2O_2 was totally consumed, so maximum COD removal was surely achieved for a set of reaction variables values.

2.2.2. Photo-Fenton process

The UV-assisted Fenton treatment of the sampled RO retentate was optimized following the same experimental procedure just describe above, plus a 450W high-pressure mercury immersion lamp (ACE-glass, Model 7825-34, Vineland, USA) assisted the Fenton process. This lamp was located vertically in the centre of the reactor enclosed inside a quartz glass vessel through which water was circulated to reduce excessive heat generated during irradiation. In addition, cooling water flowing through the double-walled immersion well eliminated the infrared spectrum of the light. The entire

assembly was kept inside a photochemical safety cabinet (ACE-glass, Vineland, USA). The total power radiated in the visible and UV regions was 159.4W (47.5% and 52.5% respectively). Major emission bands (>3%) were located at 578.0 nm (12.5%); 546.1 nm (15.4%); 435.8 nm (12.7%); 404.5 nm (6.9%); 366.0 nm (16.1%); 313.0 nm (8.3%); 302.5 nm (4.5%); 253.7 nm (3.6%). A total photon flux in the photochemical reactor of $1.1 \cdot 10^{20}$ photons/s was calculated as described in Liang et al. (2011). Light intensity was recorded using a radiometer (UV-Elektronik , UV-VIS Radiometer RM-21, Ettlingen, Germany), resulting in 186mW/cm^2 between 315 to 400 nm, at the mid-height of the UV-lamp, and 1.5 cm from the light source, which was the distance between sample and irradiation source. The UV-lamp was switched on just before H_2O_2 was added (reaction time = 0).

2.2.3. Photocatalysis

Photocatalytic treatment was performed using a similar experimental procedure and the same UV-lamp equipment just described for the photo-Fenton process despite no H_2O_2 was added to promote HO• generation, and TiO_2 (AEROXIDE® TIO_2 P 25, Evonik Degussa GmbH, Essen, Germany; BET surface area = 50 m^2/g; pore volume = 0.25 m^3/g, and mean particle size of ca. 30 nm) was used as reaction catalyst instead Fe^{2+}. Although several semiconductor catalysts have been proved to increase the treatment efficiency of UV light, TiO_2 has received much greater attention in photocatalysis technology research and development initiatives (Chong et al., 2010); and it has been particularly reported that TiO_2 is more efficient than ZnO, whether immobilized on glass or not (Yeber et al., 1999; 2000). Considering that photocatalytic processes performed with suspended catalysts have furthermore resulted as efficient as when they

are supported, which might even require a longer reaction time (Chong et al., 2010; Yeber et al., 1999; 2000), it was finally designed to perform the treatment with suspended TiO_2. The concentration of TiO_2 and reaction time were optimized keeping a constant pH (as received, pH = 7.5) and temperature (T = 25 ºC). These values of pH and temperature have been reported to produce optimum results previously (Chang et al., 2004; Merayo et al., 2010), and they imply significant savings on reagents consumption and heating energy. The suspension was first stirred in the dark for 10 min before irradiation (reaction time = 0). This was sufficient to reach an equilibrated adsorption as deduced from the steady state concentrations. Subsequently the UV-lamp was switched on.

Considering that this photocatalytic process may be an interesting pre-oxidation step preceding biological treatment (Yeber et al., 2000), Zahn-Wellens/EMPA Test (U. S. EPA. 712-C-98-084, 1998) was used to determine the inherent biodegradability of the resulting solution after performing TiO_2-photocatalytic treatment to the sampled RO retentate. In short, a mixture containing the test substance, mineral nutrients and activated sludge in aqueous medium is shook and aerated at 20-25 ºC under diffuse light for up to 28 days of incubation. 7-days-old activated sludge was collected from the wastewater treatment plant located in the mill. Blank controls containing activated sludge and mineral nutrients but no test substance were run in parallel. This biodegradation process was monitored measuring COD in filtered subsamples until the maximum reduction of the COD was achieved. The functional power of the activated sludge was checked running a parallel test using ethylene glycol as a reference substance, which biodegradability achieved at least a 70% COD removal within 14 days

of incubation. The ratio of the removed COD, corrected considering control results, to the initial COD value provides the percentage of biodegradation over time.

2.3. Experimental design

Response surface methodology (RSM) was used to assess the influence of the considered reaction variables as well as its interactive effect (Mason et al., 2003; Torrades et al., 2011; Wu et al., 2010) in order to optimize the Fenton and photo-Fenton treatments of RO retentate. RSM allows determining the optimal operation conditions for the reaction whether at least enclose the range of values satisfying operating specifications (Dopar et al., 2010; Wu et al., 2010; Zhu et al. 2011). Experimental design, regressions and response surfaces were calculated by SYSTAT 13 (SYSTAT Software Inc., Chicago, USA). As TiO_2 concentration and reaction time were the only two variables considered in the photocatalytic treatment, there was no need to run RSM to optimize the process.

Provided reaction time is dependent of the concentration of reagents, this variable was optimized leaving enough time to achieve asymptotical treatment efficiency in terms of removal of the COD (Hermosilla et al., 2009b; Zhang et al., 2005). As a reference, the theoretical stoichiometrical relation between the COD and the required H_2O_2 quantity to generate enough HO• to totally oxidize the organic matter is 2.125 (Kim et al., 1997), although a higher optimum value is expected due to parallel reactions and inefficiencies of the process (Hermosilla et al., 2009b; Pignatello et al., 2006). In addition, recent research has well stated that a $[H_2O_2]/[Fe^{2+}]$ molar ratio of 1.5, which also considers process efficiency losses, and a pH value of 2.8, produce optimum results for the Fenton treatment of other highly concentrated streams

(Hermosilla et al., 2009b; Zhang et al., 2005). Therefore, RSM was performed considering H_2O_2 concentration levels of 1.0625, 2.125 and 4.250 x initial COD value (mg/L); $[H_2O_2]/[Fe^{2+}]$ molar ratios of 1.0, 1.5 and 2.0 for the Fenton treatment, and up to 30 for the photo-Fenton treatment. $[Fe^{2+}]$ present in the effluent (Table 1) was considered in the calculations. Hermosilla et al., (2009b) reported up to a 32 times lower use of $FeSO_4$ thanks to the photo-regeneration of Fe^{2+} from Fe^{3+}); and pH values of 2.8, 5.0 and 7.2. It is of particular interest assessing whether shifting to closer values to the natural pH value of the treated stream (7.5 ± 0.5; Table 1) may not suppose great treatment efficiency losses. All experiments were repeated three times.

RSM regression analysis was performed according to a full factorial design (N=27) using the following quadratic model:

$$Y = b_0 + \sum_{i=1}^{k} b_i X_i + \sum_{i=1}^{k} b_{ii} X_i^2 + \sum_{i=1}^{k} \sum_{j=1}^{k} b_{ij} X_i X_j$$

Where Y (COD removal) is the process response dependent variable, X_i are the considered independent variables ($X_1 = [H_2O_2]/COD$; $X_2 = [H_2O_2]/[Fe^{2+}]$: $X_3 = pH$); and b_i, b_{ii} and b_{ij} are the corresponding regression coefficients.

3. Results and discussion

The application of RSM multiple regression analysis to Fenton process results produced the following quadratic model: $COD = 59.244 + 17.935 \cdot X_1 + 22.189 \cdot X_2 - 8.052 \cdot X_3 - 1.969 \cdot X_1^2 - 6.721 \cdot X_2^2 + 0.556 \cdot X_3^2 - 0.191 \cdot X_1 \cdot X_2 - 0.519 \cdot X_1 \cdot X_3 - 0.549 \cdot X_2 \cdot X_3$. This model resulted highly significant ($F=20.44$; $p<0.001$), and the prediction accuracy of the model in terms of the multiple R of the regression was 0.957. The corresponding model generated for the results of the performed photo-Fenton trials was: $COD = 60.215 + 34.775 \cdot X_1 + 0.555 \cdot X_2 - 8.210 \cdot X_3 - 4.610 \cdot X_1^2 + 0.024 \cdot X_2^2 + 0.539 \cdot X_3^2 + 0.039 \cdot X_1 \cdot X_2 -$

1.100·X_1·X_3 - 0.351·X_2·X_3. Prediction accuracy and significance of this model were also very high (multiple R of the regression = 0.974, F=35.07, $p<0.001$)

3.1. Conventional Fenton treatment

3.1.1. Assessing the effect of pH

pH has been addressed as one of the main factors limiting the performance of the Fenton treatment of wastewater, playing a major role in the control of the activity of the oxidant and the substrate, the stability of H_2O_2 itself, and the speciation of iron (Gulsen and Turan, 2004; Hermosilla et al., 2009b; Zhang et al., 2005). As pH increases, iron precipitates as $Fe(OH)_3$ (Kiwi et al., 1993), and H_2O_2 is decomposed to oxygen (Pulgarin and Kiwi, 1996). On the other hand, when pH is less than 4, inorganic carbon can be also removed, limiting its HO• scavenging activity (Buxton et al., 1988), and the solubility of iron increases (Kiwi et al., 1993), improving the overall efficiency of the process. In addition, a continuous pH control operation along the treatment usually implies a higher economical cost and causes the conductivity of the solution to rise. Therefore, the limit for effluent conductivity set by current environmental legislation may limit its disposal.

The designed RSM identified pH=2.8 as the optimal value for the Fenton treatment of the sampled RO retentate from the paper mill (Figure 1), which has been also reported optimal previously for the performance of this treatment to landfill leachate (Hermosilla et al., 2009b) and phenol (Kavitha and Palanivelu, 2004) . In addition, it is important to consider the possibility of implementing this process at natural effluent pH values, which is close to neutral (pH ≈ 7.5, Table 1); therefore avoiding an extra cost for controlling the pH, and potential trouble that may be caused

by an increased effluent conductivity. In fact, reasonable reductions of the COD (60-70%) were achieved working from an initial pH = 7.2, but at higher reagents dosage (Figure 1).

pH decreased naturally to 2.8 along the reaction when the initial value in the solution was higher, up to neutral (Figure 2), an effect that has been previously attributed to the production of CO_2 and fatty organic acids as other organic compounds are oxidized (Hermosilla et al., 2009a). This way, the influence of an initial higher pH value than the optimum is partially compensated by an increase in the consumption of H_2O_2; but certain oxidation efficiency loss is always addressed due to the decomposition of the oxidants, a lower solubility of iron, and parallel reactions (Gulsen and Turan, 2004; Pulgarin and Kiwi, 1996; Zhang et al., 2005).

3.1.2. Optimizing the required quantity of reagents

The use of chemical reagents is a major operational cost item when implementing Fenton treatment facilities for industrial wastewater (Gulsen and Turan, 2004; Zhang et al., 2005). Reagents dosage requirements were properly assessed by RSM in terms of the relative amount of H_2O_2 required per COD unit, and the molar ratio between H_2O_2 and Fe^{2+} (Figure 1 and 3). Results were in good agreement with those previously reported for other highly organic loaded wastewater (Hermosilla et al., 2009a; Rivas et al., 2003; Torrades et al., 2011; Zhang et al., 2005). Accordingly, although a 1:1 molar ratio between H_2O_2 and Fe^{2+} corresponds to the theoretical optimal stoichiometry for the formation of $HO\bullet$ in a Fenton reaction (Harber and Weiss, 1934), the better operation conditions were provided by ≈1.5 values regardless the initial pH value of the reaction (as shown in Figure 3), reflecting a net oxidation efficiency loss through parallel

reactions (≈33%). Particularly, H_2O_2 is able to reduce Fe^{3+} back to Fe^{2+}, recovering catalyst for further HO• generation, although this process is several orders of magnitude slower than the direct HO• production by Fenton reagents (Hermosilla et al., 2009b; Pignatello et al., 2006).

The optimal H_2O_2 concentration resulted about 3.8 times the initial COD value, although the additional removal of COD was <5% over 2.8 (Figure 3). This is 0.675-1.675 times greater than the theoretical optimal stoichiometrical ratio of 2.125 mg $H_2O_2 \cdot L^{-1}$ for every COD $mgO_2 \cdot L^{-1}$ (Kim et al., 1997). Previous research reported slightly lower values (2.15-2.40) for the Fenton treatment of phenol (Kavitha and Palanivelu, 2004), brines (Rivas et al., 2003), and black liquor from pulp and paper industry (Torrades et al., 2011); whereas an even higher inefficiency of the added H_2O_2 was found for highly organic-loaded stabilized landfill leachate (Hermosilla et al., 2009b).

Particularly, the use of Fenton treatment for 100% recovered paper newsprint mill effluents has not been reported before. Moreover, available results for the conventional Fenton treatment of wastewater from other paper mills are very limited, and may have not even been optimized. Comparatively, the reduction level of the COD that has been achieved in the performed optimal Fenton treatment of RO retentate from this paper mill is even higher (>80-90%; Figure 1) than the best reported for other paper mill effluents (30-85%; Catalkaya and Kargi, 2007; Sevimli, 2005; Tambosi et al., 2006). The percentage of TOC removed for the best treatment conditions was 50-60%, which represents a high mineralization ratio for the removed COD, similar to previously reported results for the Fenton treatment of other complex wastewater (Hermosilla et al., 2009b). The fact that coagulation may significantly contribute to remove organic load

when a Fenton process is performed at high iron dosages (Kang and Hwang, 2000) may in part explain these very good COD and TOC removal results.

3.2. Photo-Fenton treatment

As Fenton reaction progresses, recalcitrant organic byproducts may be generated, such as some carboxylic acids and fatty acids, as well as organic iron-complexes that hinder the process (Hermosilla et al., 2009a). Particularly, it has been reported that the Fenton treatment of acid fractions from starch degradation is only able to achieve a 3% COD removal, which has been attributed to their organic structure (Amat et al., 2005). These limitations may be widely avoided combining the application of UV-irradiation with the Fenton treatment. As it has been previously reported, a higher treatment efficiency is possible because it enables further treatment of some organics that could not be treated otherwise, and it requires the addition of much less Fe^{2+}, reducing very much turbidity and sludge generation (Hermosilla et al., 2009a; Kavitha and Palanivelu, 2004; Kim and Vogelpohl, 1998; Safarzadeh et al., 1997). The progression of the reaction is further driven by the photo-regeneration of Fe^{2+} from Fe^{3+}, and the breakage of iron complexes (Hermosilla et al., 2009a).

In fact, the optimal photo-Fenton treatment of the sampled RO retentate from the paper mill achieved a total reduction of the initial COD (Figure 4) and TOC values. The optimal photo-Fenton reaction conditions were addressed at pH = 2.8, $[H_2O_2]/COD > 2.25$, and $[H_2O_2]/[Fe^{2+}] > 10$ (Figure 4). Particularly, pH resulted to have a greater effect in the applied photo-Fenton process than when performing conventional Fenton treatment, as denoted by the much greater drop in the achieved reduction of the COD at higher pH values than the optimum (compare Figures 1 and 4). In addition, pH

increased naturally to neutral values when the photo-Fenton treatment was performed after adjusting the initial pH value at 2.8 (Figure 2). Further pH adjustment was not required as fatty organic acids were totally removed.

On the other hand, the performed optimal photo-Fenton treatment required a lower concentration of H_2O_2 to remove more COD than the above-defined optimal conventional Fenton treatment ($[H_2O_2]/COD > 2.8$; Figure 1); which denotes that Fe^{3+} to Fe^{2+} photo-reduction effectively promotes a quicker evolution of the Fenton reaction (Hermosilla et al, 2009a). In turn, the availability of Fe^{2+} becomes the main rate-limiting step of the conventional Fenton process because the regeneration of Fe^{2+} from Fe^{3+} is slower than the consumption of ferrous iron (Hermosilla et al., 2009b; Pignatello et al., 2006); therefore, more H_2O_2 is required to reach the same concentration of HO• that is produced when UV-light is assisting the reaction.

Moreover, the oxidation efficiency of the process ($OE = 100 \cdot \Delta COD/available\ O_2$, where "available O_2" matches the theoretical amount of reactive oxygen equivalent to the added H_2O_2; (Bishop et al., 1968) also deteriorates as the reaction further proceeds when Fe^{2+} regeneration by H_2O_2 becomes predominant (Hermosilla et al., 2009b). Accordingly, considering the theoretical stoichiometrical H_2O_2 concentration of 2.125 times the COD value, it results that OE is significantly greater for photo-Fenton ($OE = 0.78$) than for conventional Fenton treatment ($OE = 0.64$) at $pH = 2.8$. Finally, a much higher requirement of Fe^{2+} addition will further imply an associated higher cost for iron sludge disposal after performing the conventional Fenton treatment of RO retentate. In fact, less iron sludge generation has been reported previously when optimizing Fenton and photo-Fenton treatments of landfill leachate (Hermosilla et al. 2009b) and in this case $[H_2O_2]/[Fe^{2+}]$ ratio may be higher than 30 (Figure 4).

3.3. TiO_2-photocatalytic treatment

Although the reduction of the COD seemed to be almost maximized during the first hour of treatment, as reported previously in other similar trials (Dialynas et al., 2008), it stepped up further from 90 min onwards (Figure 5). During the first 10 minutes of treatment (UV-lamp switched off) part of the COD is adsorbed in TiO_2. It was measured that 25, 75 and 95 mgO_2/L of COD were adsorbed for 1, 5 and 10 g/L dosages of TiO_2 respectively. After switching the lamp on, easily oxidizable organics were removed; and in a second stage, organic matter was eliminated at a much slower rate (up to ≈60 min). As easier-to-oxidize byproducts are generated from the treatment of more recalcitrant chemicals, a higher COD removal can be achieved. Similar successive stages may alternate prolonging the process indefinitely, so a 5 hours treatment was set as a reasonable reference to compare results. Further treatment did not seem to add significant reduction of the COD for the investment of such an extra reaction time and cost (Figure 5).

The overall efficiency of the process was strongly influenced by the dosage of TiO_2 (Figures 5 and 6), as it has been reported previously (Chang et al., 2004; Tanaka et al., 1999). The degradation of organics is improved until an excessive catalyst dosage causes a shadow effect interfering with the transmission of UV light, so electron-hole pairs generation cannot effectively occur (Catalkaya and Kargi, 2007; Chang et al., 2004). An optimum dosage of 10 $g \cdot L^{-1}$ of TiO_2 was found to maximize the removal of COD (35-40%) and TOC (30-35%) after a 5-hour TiO_2-photocatalytic treatment of the sampled RO retentate (Figure 6), as it has been previously reported for the equivalent treatment of lignin powder (Chang et al., 2004). Although the removal of COD is not

much better (≈ 5%) than using 5 g[TiO_2]·L^{-1} , the mineralization of the organic fraction was much enhanced (> 2 times). These COD removal ranking results are similar to those reported comparing TiO_2-photocatalytic and solar photo-Fenton treatments of effluents from board industry (Amat et al., 2005).The shown limited efficiency of TiO_2-photocatalyisis was attributed to the lower oxidative power this treatment developed in comparison to the previously applied Fenton processes, as reflected by the evolution of the measured redox potential along the reaction time. While redox potential raised pretty quickly during the first 2 minutes of Fenton and photo-Fenton processes from an initial value of 400 RmV to final values of 530 and 550 RmV, respectively; its evolution was more progressive along the photocatalytic treatment, beginning at -100 Rm V, and still increasing more or less linearly after reaching 55 RmV after a 3-h trial.

Beyond these overall poorer oxidative results, it has furthermore been highlighted that the photocatalytic degradation of organics mainly affected those pollutants that are more reluctant to biological degradation, thus enhancing much the biodegradability of wastewater (Amat et al., 2005; Yeber et al., 2000). Particularly, it has been shown that it may be able to reduce over the 30% content of high molecular weight compounds present in cellulose bleaching effluents (Yeber et al., 2000). Therefore, TiO_2-photocatalysis may be considered as an interesting pre-oxidation step preceding biological treatment of paper industry wastewater. In fact, biodegradability was improved along the TiO_2-photocatalytic treatment of RO retentate, even achieving close figures to those developed by ethylene glycol (≈100% COD removal) when 10 g·L^{-1} of TiO_2 were used (Figure 7).

3.4. Some considerations regarding the cost of the treatments.

Considering a first tentative economical assessment of the cost of the tested treatments, it could be easily understood that, whereas the conventional Fenton treatment implies a higher cost in terms of chemical reagents, which will furthermore imply an associated higher cost for iron sludge disposal as well; the photo-Fenton treatment requires a higher cost in terms of energy consumption. In short, a first estimation of the treatment cost in terms of reagents and energy implied at lab scale resulted in about the same order of magnitude for both optimal Fenton (4.17 $/m^3$; calculated as described in Esplugas et al., 2002) and photo-Fenton (3.63 $/m^3$) treatments yielding a 70% COD removal; resulting the latter much interesting if we consider that it is even able to produce a 100% reduction of the COD, its much lower associated cost for iron sludge disposal, and the potential use of a solar source of radiation to substitute UV lamps and save from the associated cost of energy whenever possible.

On the other hand, TiO_2-photocatalytic treatment showed more than a half lower COD and TOC removal figures at best, requiring very long treatment times, and therefore increasing much the use of UV-lamps and the associated cost of energy (up to 74.80 $/m^3$ for a 33% COD reduction). As much longer time (up to 5 hours) was required for producing the same COD removal target than photo-Fenton (5 minutes), photocatalysis may could only represent an interesting treatment alternative whenever it would be possible to use the sun as an alternative source for radiation, which application may be further limited for high effluent flows (3000 m^3/day) by an increased residence time and its associated operational cost.

4. Conclusions

• The photo-Fenton process was the most effective among the tested treatments for RO retentate from a paper mill, achieving the total reduction of COD and TOC. Furthermore, it was cheaper than conventional Fenton at higher COD reduction treatment thresholds.

• In addition, although better results were produced when the initial pH value was pre-adjusted to 2.8, Fenton processes were able to achieve acceptable high COD reduction results (> 60%) without adjusting the initial pH value of the solution, which is close to neutral.

• TiO_2-photocatalysis increased the biodegradability of the highly concentrated RO retentate enough to consider its combination with a posterior biological step in order to achieve an almost total reduction of the COD. A solar version of this process might reduce much the high energy cost that has been associated to this treatment.

Acknowledgments

This research was developed in the frame of the projects "AQUAFIT4USE" (211534), funded by the European Union; "AGUA Y ENERGÍA" (CTM2008-06886-C02-01), and "OXIPAPEL" (CIT-310000-2008-15), both funded by the Ministry of Science and Innovation of Spain; and "PROLIPAPEL II" (P-2009/AMB/1480) funded by the Community of Madrid.

References

Amat, A.M., Arques, A., López, F., Miranda, M.A., 2005. Solar photo-catalysis to remove paper mill wastewater pollutants. Sol. Energy 79, 393-401.

APHA, AWWA, WPCF (Eds.), 2005. Standard methods for the examination of water and wastewater, Washington DC.

Asano, T., Cotruvo, J.A., 2004. Groundwater recharge with reclaimed municipal wastewater: health and regulatory considerations. Water Res. 38, 1941-1951.

Bishop, D.F., Stern, G., Fleischman, M., Marshall, L.S., 1968. Hydrogen peroxide catalytic oxidation of refractory organics in municipal wastewaters. I & EC Process Design and Development 7, 110-117.

BREF, Integrated Pollution Prevention and Control (IPPC): Reference Document on Best Available Techniques in the Pulp and Paper Industry; European Commission: 2011.

Buxton, G.V., Greenstock, C.L., Helman, W.P., Ross, A.B., 1988. Critical review of rate constants for reactions of hydrated electrons, hydrogen-atoms and hydroxyl radicals (·OH/·O-) in aqueous-solution. J. Phys. Chem. 17, 513-886.

Catalkaya, E.C., Kargi, F., 2007. Color, TOC and AOX removals from pulp mill effluent by advanced oxidation processes: A comparative study. J. Hazard. Mater. 139, 244-253.

Chang, C.N., Ma, Y.S., Fang, G.C., Chao, A.C., Tsai, M.C., Sung, H.F., 2004. Decolorizing of lignin wastewater using the photochemical UV/TiO_2 process. Chemosphere 56, 1011-1017.

Chong, M.N., Jin, B., Chow, C.W.K., Saint, C., 2010. Recent developments in photocatalytic water treatment technology: A review. Water Res. 44, 2997-3027.

Dialynas, E., Mantzavinos, D., Diamadopoulos, E., 2008. Advanced treatment of the reverse osmosis concentrate produced during reclamation of municipal wastewater. Water Res. 42 (18), 4603-4608.

Dopar, M., Kusic, H., Koprivana, N., 2010. Treatment of simulated industrial wastewater by photo-Fenton process. Part I: The optimization of process parameters using design of experiments (DOE). Chem. Eng. J. (*in press).*

Esplugas, S., Giménez, J., Contreras, S., Pascual, E., Rodríguez, M., 2002. Comparison of different advanced oxidation processes for phenol degradation. Water Res. 36, 1034-1042.

Greenlee, L.F., Testa, F., Lawler, D.F., Freeman, B.D., Moulin, P., 2010a. The effect of antiscalant addition on calcium carbonate precipitation for a simplified synthetic brackish water reverse osmosis concentrate. Water Res. 44 (9), 2957-2969.

Greenlee, L.F., Testa, F., Lawler, D.F., Freeman, B.D., Moulin, P., 2010b. Effect of antiscalants on precipitation of an RO concentrate: Metals precipitated and particle characteristics for several water compositions. Water Res. 44 (8), 2672-2684.

Gulsen, H., Turan, M., 2004. Treatment of sanitary landfill leachate using a combined anaerobic fluidized bed reactor and Fenton's oxidation. Environ. Eng. Sci. 21, 627-636.

Hermosilla, D., Cortijo, M., Huang, C.P., 2009a. The role of iron on the degradation and mineralization of organic compounds using conventional Fenton and photo-Fenton processes. Chem. Eng. J. 155, 637–646.

Hermosilla, D., Cortijo, M., Huang, C.P., 2009b. Optimizing the treatment of landfill leachate by conventional Fenton and photo-Fenton processes. Sci. Total Environ. 407, 3473–3481.

Hoffmann, M.R., Martin, S.T., Choi, W.Y., Bahnemann, D.W., 1995. Environmental applications of semiconductor photocatalysis. Chem. Rev. 95, 69-96.

1 Kang, Y.W., Hwang, K., 2000. Effects of reaction conditions on the oxidation
2 efficiency in the Fenton process. Water Res. 34, 2786-2790.
3 Kavitha, V., Palanivelu, K., 2004. The role of ferrous ion in Fenton and photo-Fenton
4 processes for the degradation of phenol. Chemosphere 55, 1235-1243.
5 Kim, S., Geissen, S., Vogelpohl, A., 1997. Landfill leachate treatment by a
6 photoassisted Fenton reaction. Water Sci. Technol. 35, 239-248.
7 Kim, S., Vogelpohl, A., 1998. Degradation of organic pollutants by the photo-Fenton-
8 process. Chem. Eng. Technol. 21, 187-191.
9 Kiwi, J., Pulgarin, C., Peringer, P., Gratzel, M., 1993. Beneficial effects of
10 homogeneous photo-Fenton pretreatment upon the biodegradation of anthraquinone
11 sulfonate in waste-water treatment. Appl. Catal. B 3, 85-99.
12 Koppol, A.R., Bagajewicz, M.J., Dericks, B.J., Savelski, M.J., 2004. On zero water
13 discharge solutions in the process industry. Adv. Environ. Res. 8, 151-171.
14 Kuhn, H. J., Braslavsky, S.E., Schmidt, R., 2004. Chemical Actinometry. Pure Appl.
15 Chem. 76, (12), 2105–2146.
16 Liang, X., Zhu, X., Butler, E.C., 2011. Comparison of four advanced oxidation
17 processes for the removal of naphthenic acids from model oil sands process water. J.
18 Hazard. Mater. 190, 168-176.
19 Mason, R.L., Gunst, R.F., Hess, J.L., 2003. Statistical design and analysis of
20 experiments, eight applications to engineering and science, second ed., Wiley, New
21 York.
22 Merayo, M., Hermosilla, D., Blanco, L., Blanco, A., 2010. Photocatalysis and ozone
23 treatment of pulp and paper mill effluents. In: Proceedings of the 7th Anque's
24 International Congress, Oviedo, Asturias, Spain.

Mobius, C.H., Helble, A., 2004. Combined ozonation and biofilm treatment for reuse of papermill wastewaters. Water Sci. Technol. 49, 319-323.

Muñoz, I., Rieradevall, J., Torrades, F., Peral, J., Doménech, X., 2006. Environmental assessment of different advanced oxidation processes applied to a bleaching Kraft mill effluent. Chemosphere 62, 9-16.

Ning, R.Y., Troyer, T.L., 2009. Tandom reverse osmosis process for zero-liquid discharge. Desalination 237, 238-242.

Oller, I., Malato, S., Sánchez-Pérez, J.A., 2011. Combination of Advanced Oxidation Processes and biological treatments for wastewater decontamination—A review. Sci. Total Environ. 409, 4141–4166.

Ordoñez, R, Hermosilla, D., Fuente, E., Blanco, A., 2009. Influence of water quality on the efficiency of retention aids systems for the paper industry. Ind. Eng. Chem. Res. 48, 10247–10252.

Ordoñez, R., Hermosilla, D., San Pío, I., Blanco, A., 2010. Replacement of fresh water use by final effluent recovery in a highly optimized 100% recovered paper mill. Water Sci. Technol. 62, 1694-1703.

Pignatello, J.J., Oliveros, E., MacKay, A., 2006. Advanced oxidation processes for organic contaminant destruction based on the Fenton reaction and related chemistry. Crit. Rev. Environ. Sci. Technol. 36, 1–84.

Pobiner, H., 1961. Determination of hydroperoxides in hydrocarbon by conversion to hydrogen peroxide and measurement by titanium complexing. Anal. Chem. 33, 1423-1428.

Pulgarin, C., Kiwi, J., 1996. Overview on photocatalytic and electrocatalytic pretreatment of industrial non-biodegradable pollutants and pesticides. Chimia 50, 50-55.

Rivas, F.J., Beltran, F.J., Gimeno, O., Alvarez, P., 2003. Treatment of brines by combined Fenton's reagent-aerobic biodegradation II. Process modeling. J. Hazard. Mater. B96, 259-276.

Rivas, F.J., Frades, J., Alonso, M.A., Montoya, C., Monteagudo, J.M., 2005. Fenton´s oxidation of food processing wastewater components. Kinetic modelling of protocatechuic acid degradation. J. Agric. Food Chem. 53, 10097-10104.

Safarzadeh, A., Bolton, J.R., Cater, S.R., 1997. Ferrioxalate-mediated photodegradation of organic pollutants in contaminated water. Water Res. 31, 787-798.

Sevimli M.F., 2005. Post-treatment of pulp and paper industry wastewater by advanced oxidation processes. Ozone-Sci. Eng. 27, 37-43.

Sundholm, P., 2000. Mill operations in production of main paper and board grades. In Paulupuro H editor. Papermaking Science and Technology, book 8: Papermaking, Part 1, Stock Preparation and Wet End. 1st Edition Jyväskylä, Finland Gummerus, 2000, 11-55.

Tambosi, J.L., Di Domenico, M., Schirmer, W.N., Jose, H.J., Moreira, R.D.P.M., 2006. Treatment of paper and pulp wastewater and removal of odorous compounds by a Fenton-like process at the pilot scale. J. Chem. Technol. Biotechnol. 81, 1426-1432.

Tamura, H., Goto, K., Yotsuyanagi, T., Nagayama, M., 1974. Spectrophotometric determination of iron (II) with 1,10-phenanthroline in the presence of large amounts of iron (III). Talanta 21, 314-318.

Tanaka, K., Calanag, R.C.R., Hisanaga, T., 1999. Photocatalyzed degradation of lignin on TiO_2. J. Mol. Catal. A 138, 287-294.

Torrades, F., Saiz, S., Garcia-Hortal, J.A., 2011. Using central composite experimental design to optimize the degradation of black liquor by Fenton reagent. Desalination, 268, 97-102.

U. S. EPA. 712-C-98-084. 1998. Fate, Transport and yransformation test guidelines. OPPTS 835.3200 Zahn-Wellens/EMPA Test.

Wu, Y., Zhou, S., Qin, F., Ye, X., Zheng, K., 2010. Modeling physical and oxidative removal properties of Fenton process for treatment of landfill leachate using response surface methodology (RSM). J. Hazard. Mater. 180, 456-465.

Yeber, M.C., Rodríguez, J., Freer, J., Baeza, J., Duran, N., Mansilla, H.D., 1999. Advanced oxidation of a pulp mill bleaching wastewater. Chemosphere 39, 1679-1688.

Yeber, M.C., Rodríguez, J., Freer, J., Duran, N., Mansilla, H.D., 2000. Photocatalytic degradation of cellulose bleaching effluent by supported TiO_2 and ZnO. Chemosphere 41, 1193-1197.

Zhang, H., Choi, H.J., Huang, C.P., 2005. Optimization of Fenton process for the treatment of landfill leachate. J. Hazard. Mater.125, 166-174.

Zhu, X., Tian, J., Liu, R., Chen, L., 2011. Optimization of Fenton and electro-Fenton oxidation of biologically treated coking wastewater using response surface methodology. Sep. Purif. Technol. 81, 444–450.

Table 1. Chemical characterization of the treated RO retentate from a paper mill.

Parameter	units	average	standard deviation
Temperature	ºC	23	2
pH		7.5	0.5
CODt	mg/L	530	74
TOC	mg/L	111	13
BOD_5	mg/L	21	4
TSS	mg/L	21	7
Conductivity	µS/cm	3679	564
Alkalinity	mg $CaCO_3$/L	750	0
P-total	mg/L	12	5
N-total	mg/L	105	22
NH_4^+-N	mg/L	17	1
NO_3^-	mg/L	45	16
Cl^-	mg/L	197	30
SO_4^{2-}	mg/L	460	19
SiO_2	mg/L	190	11
F^-	mg/L	0.28	0.11
B	mg/L	0.86	0.03
Al	mg/L	0.06	0.00
K	mg/L	18	0.60
Na	mg/L	871	97
Mg	mg/L	8	0.55
Ca	mg/L	97	7
Fe^{2+}	mg/L	1.86	1.18
Fe-total	mg/L	1.87	0.08

Fig. 1. Response surface and contour plot for the removal of COD from paper mill RO retentate by Fenton treatment considering variable pH and reagents concentrations (T = 25ºC).

Fig. 2. Evolution of pH from different adjusted initial values along Fenton and photo-Fenton treatment of RO retentate from a paper mill. Reaction variables: T = 25ºC; $[H_2O_2]/COD\ (mg \cdot L^{-1}) = 2.125$; $[H_2O_2]/[Fe^{2+}] = 1.5$ (Fenton) and 15 (Photo-Fenton).

Fig. 3. Response surface and contour plot for COD reduction from paper mill RO retentate by Fenton treatment considering variable reagents concentrations (T = 25ºC).

Fig. 4. Response surface and contour plot for COD removal from paper mill RO retentate by photo-Fenton treatment at T=25ºC and variable concentrations of reagents considering (**A**) initial pH = 2.8; and (**B**) variable both pH and H_2O_2 concentration.

Fig. 5. Reduction of the COD along reaction time when performing the treatment of RO retentate from a newsprint paper mill by TiO_2-photocatalysis at different concentration levels of the catalyst (T = 25ºC, initial natural RO-retentate pH value after the addition of the catalyst = 7.2)

Fig. 6. TiO_2-photocatalysis efficiency in the treatment of RO retentate at different concentration values of the catalyst (T = 25ºC, initial natural RO-retentate pH value after the addition of the catalyst = 7.2, reaction time = 300 minutes).

Fig. 7. Biodegradability evolution along the optimal TiO_2-photocatlaytic treatment of RO retentate from a newsprint paper mill.

FIGURE 1

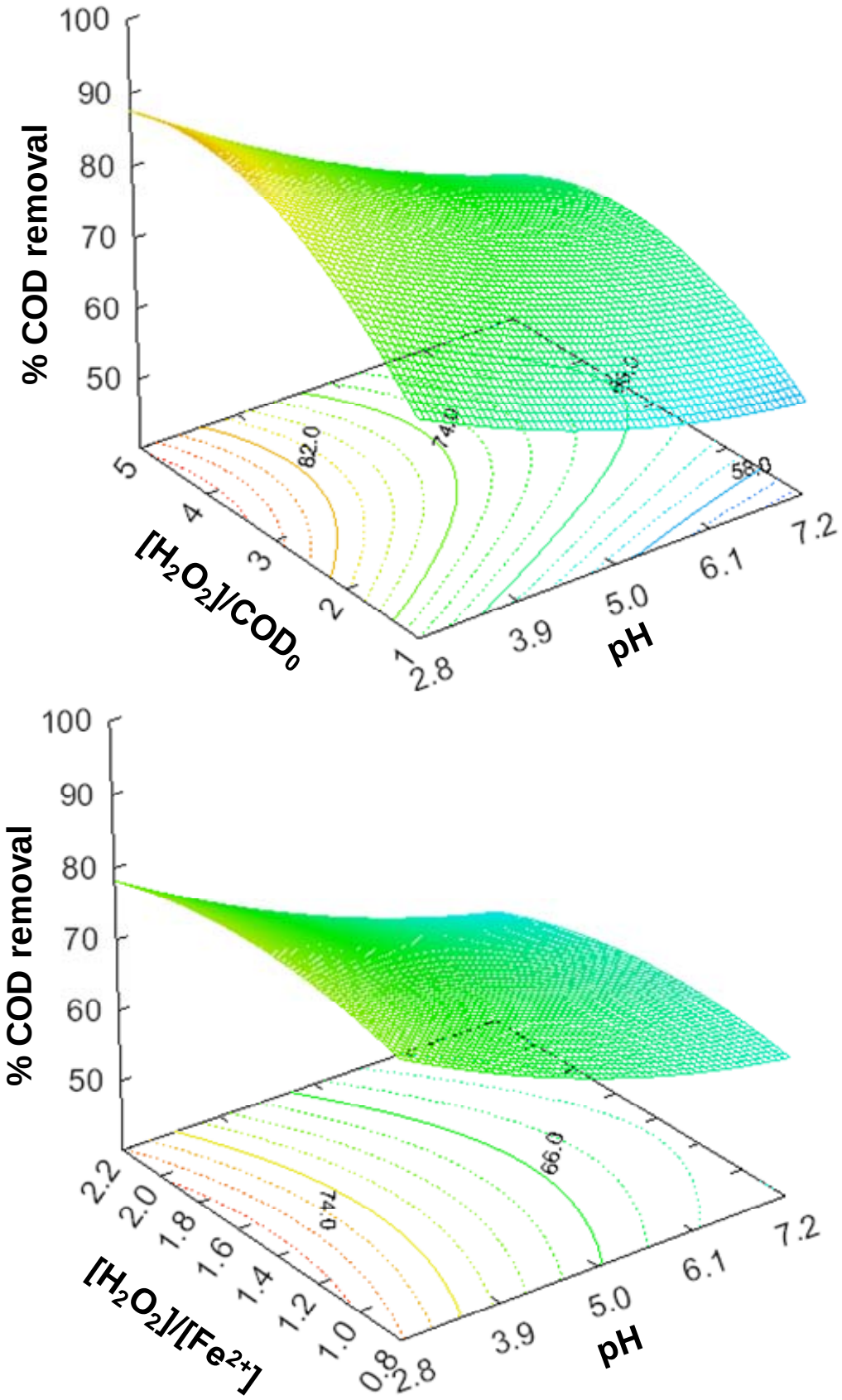
% COD removal
100
90
80
70
60
50
5
4
3
2
1
[H2O2]/COD0
2.8
3.9
5.0
6.1
7.2
pH
82.0
74.0
58.0
% COD removal
100
90
80
70
60
50
2.2
2.0
1.8
1.6
1.4
1.2
1.0
0.8
[H2O2]/[Fe2+]
2.8
3.9
5.0
6.1
7.2
pH
74.0
66.0

FIGURE 2

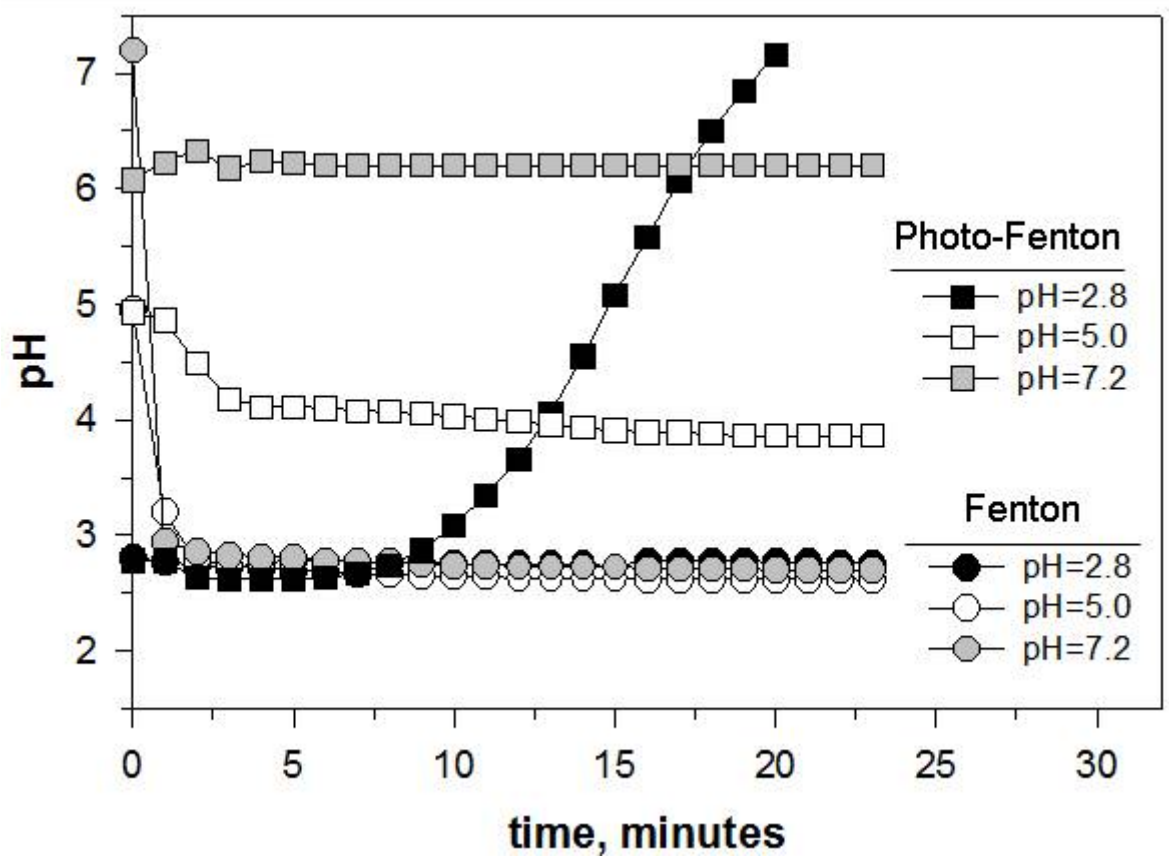
pH
time, minutes
Photo-Fenton
pH=2.8
pH=5.0
pH=7.2
Fenton
pH=2.8
pH=5.0
pH=7.2

FIGURE 3

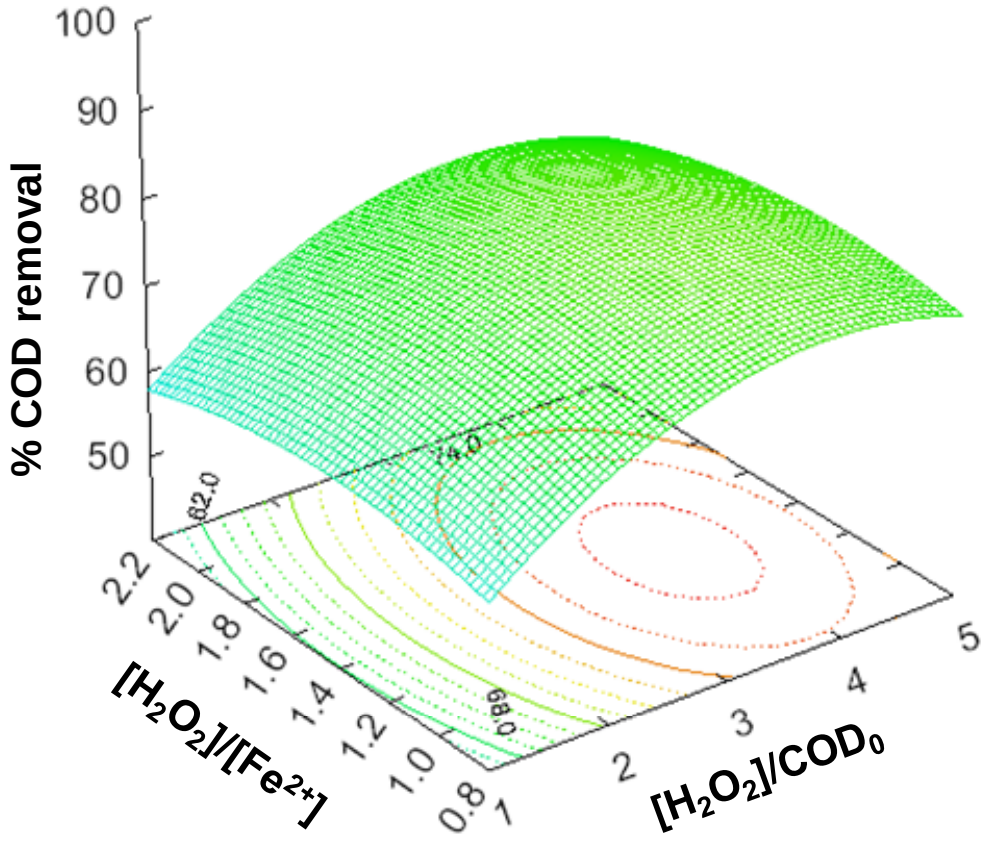
% COD removal
100
90
80
70
60
50
82.0
74.0
68.0
2.2
2.0
1.8
1.6
1.4
1.2
1.0
0.8
[H2O2]/[Fe2+]
1
2
3
4
5
[H2O2]/COD0

FIGURE 4

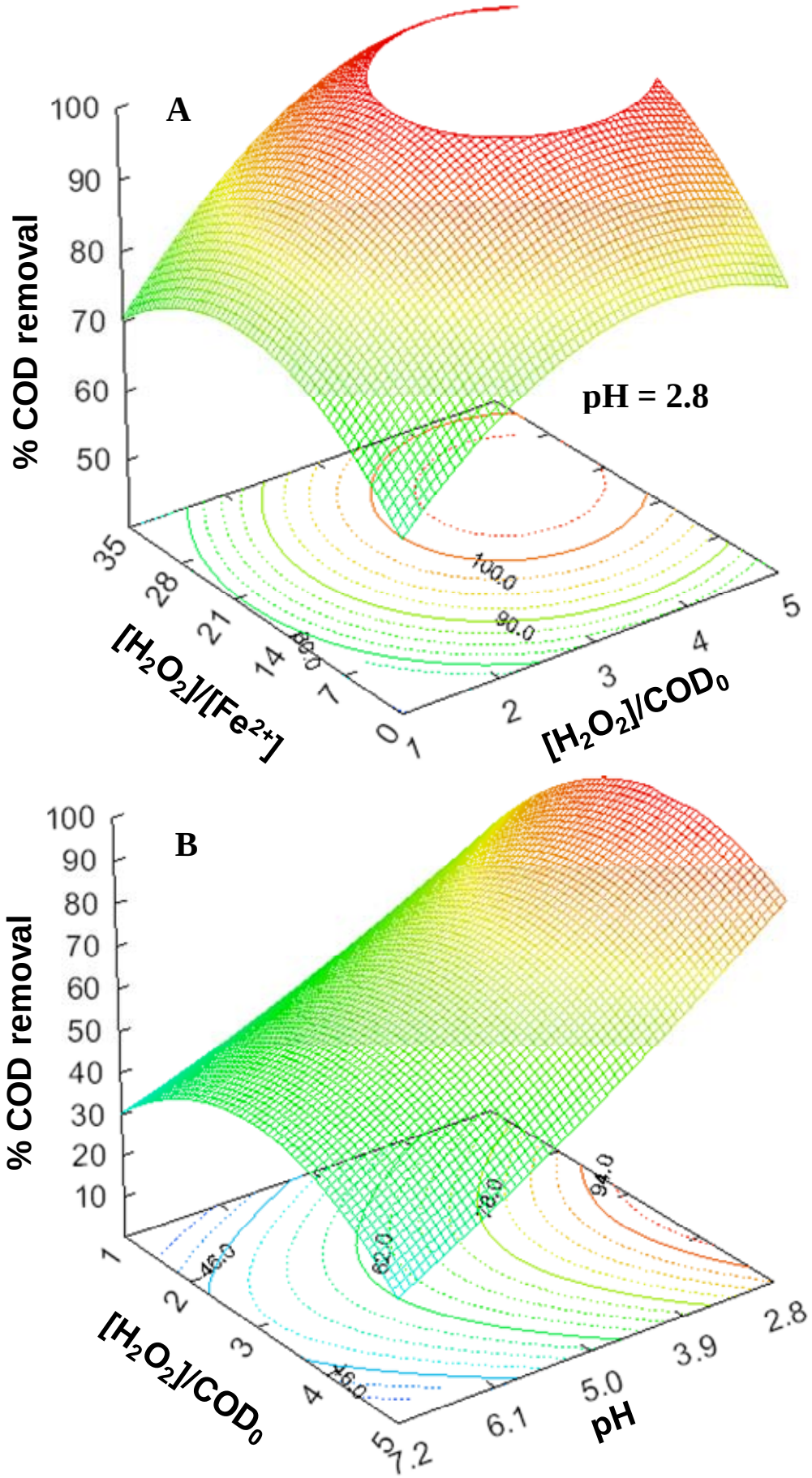
A
% COD removal
100
90
80
70
60
50
pH = 2.8
100.0
90.0
80.0
35
28
21
14
7
0
[H2O2]/[Fe2+]
1
2
3
4
5
[H2O2]/COD0
B
% COD removal
100
90
80
70
60
50
40
30
20
10
94.0
82.0
70.0
46.0
46.0
1
2
3
4
5
[H2O2]/COD0
7.2
6.1
5.0
3.9
2.8
pH

FIGURE 5

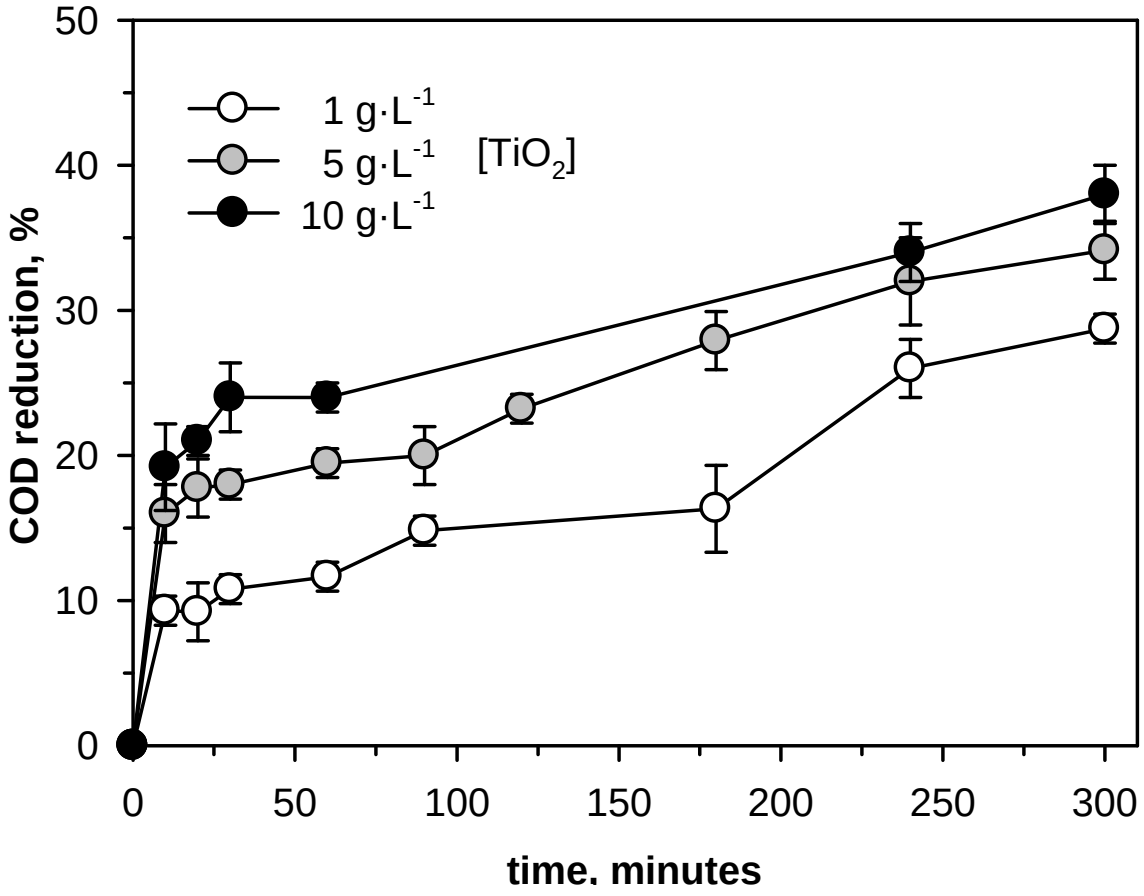
50
40
30
20
10
0
0
50
100
150
200
250
300
COD reduction, %
time. minutes
1 g·L-1
5 g·L-1
10 g·L-1
[TiO2]

FIGURE 6

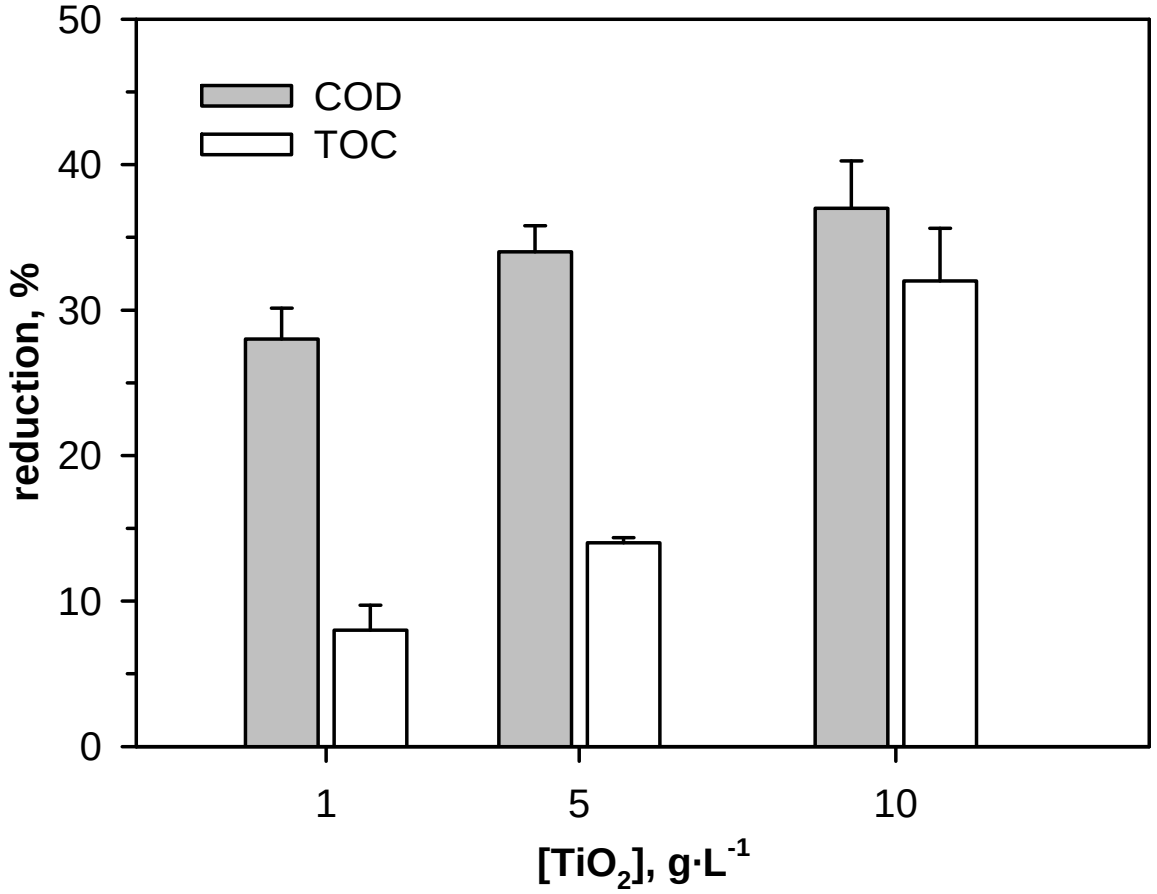

FIGURE 7

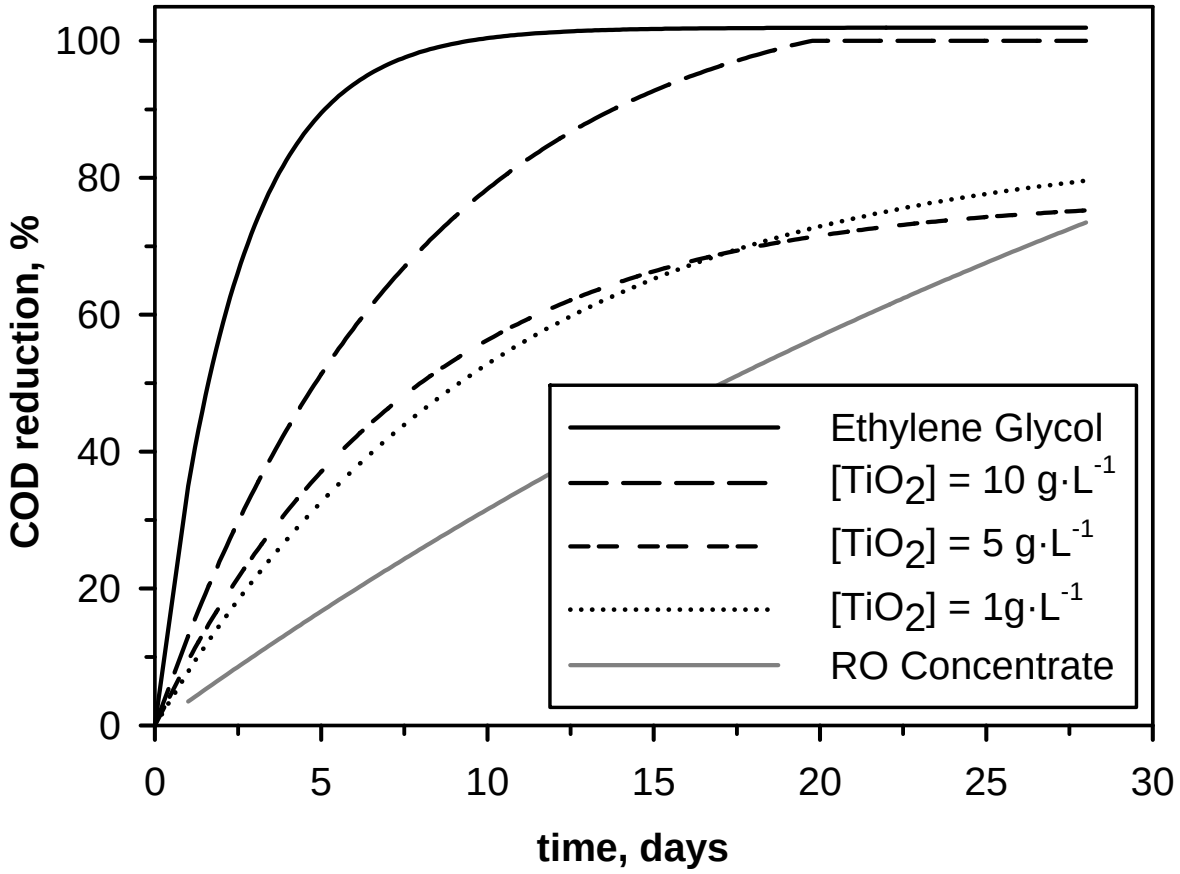
COD reduction, %
time, days
0
20
40
60
80
100
0
5
10
15
20
25
30
Ethylene Glycol
[TiO2] = 10 g·L-1
[TiO2] = 5 g·L-1
[TiO2] = 1g·L-1
RO Concentrate